Coherent Structures in a Three-dimensional Chaotic Potential Flow

L. D. Smith[1,2]**, M. Rudman**[1]**, D. R. Lester**[2]** and G. Metcalfe**[3]

[1]Department of Mechanical and Aerospace Engineering
Monash University, Clayton, VIC 3800, Australia

[2]CSIRO Computational Informatics
Clayton, VIC 3800, Australia

[3]CSIRO Materials Science and Engineering
Highett, VIC 3190, Australia

Abstract

Central to understanding all chaotic advection processes is the nature of periodic points and their associated coherent structures. They provide a framework upon which transport dynamics play out. We show that degenerate points which are often overlooked play an important role in shaping this framework and the overall flow. In particular for the three-dimensional Reoriented Potential Mixing (3DRPM) flow the degenerate points create local stable regions that prevent global chaos.

Introduction

Chaotic advection plays an important role in many physical processes and engineering applications. Chaotic advection provides an efficient and expedient method of mixing fluids, and is particularly useful in flows were turbulence is not possible. Applications of chaotic advection include small scale flows such as those in the growing field of microfluidics, flows with long time scales such as atmospheric flows, and flows in which large shear stresses would damage fragile structures such as polymers and DNA. The study of chaotic advection involves solving the advection equation

$$\dot{\mathbf{x}} = \mathbf{v}(\mathbf{x},t) \qquad (1)$$

where typically the velocity field $\mathbf{v}$ is laminar, deterministic and satisfies $\nabla \cdot \mathbf{v} = 0$, called incompressible flows. Most chaotic advection studies concern inviscid or Stokes flows and few have considered potential flows ($\mathbf{v} = \nabla \cdot \Phi$), which are important since they model homogeneous porous media flows which have applications in groundwater flows. In this study we consider only periodic flows, i.e. $\mathbf{v}(\mathbf{x},t) = \mathbf{v}(\mathbf{x},t+T)$ for some period T.

A point in a periodic flow is said to be periodic with period n if a particle returns to its starting position after n flow periods. The study of periodic points and their stability within flows with chaotic advection provides a skeleton that determines overall flow structures, predicting both chaotic and non-mixing regions [7]. In contrast to locally stable (elliptic) and locally unstable (hyperbolic) periodic points, degenerate periodic points have not been studied in the context of chaotic fluid flow. In this study we highlight the importance of degenerate points, showing that a type of degenerate point prevents chaos.

Chaotic advection in two-dimensional incompressible flows has been studied extensively in contrast to three-dimensional flows. As a result there is a discrepancy in the understanding of two-dimensional flows compared to three-dimensions [10]. A key reason for this discrepancy is that two-dimensional incompressible flows can be cast as one degree-of-freedom Hamiltonian systems. Hamiltonian theory has been extensively developed over a large period of time. However, the Hamiltonian connection breaks down for three-dimensional flows at stagnation points [1], making conversion of two-dimensional theory to three-dimensions either difficult or impossible. Furthermore, there is an explosion of geometric complexity in the transition from two dimensions to three. As an example, in two-
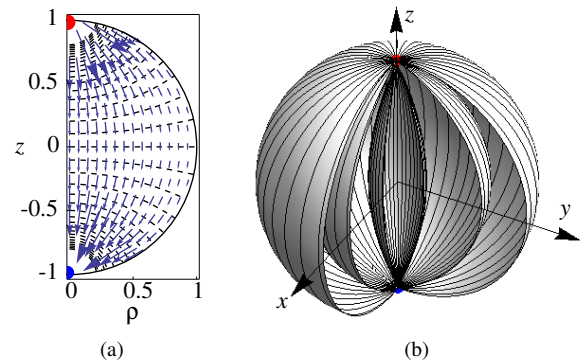

Figure 1. (a) Contours of the axisymmetric potential function Φ and velocity field $\mathbf{v}$. (b) Isosurfaces of the axisymmetric stream function Ψ.

dimensional incompressible flows periodic points can only occur as isolated points, but in three-dimensions they can either be isolated or form a continuous line. This creates many more possibilities for the associated coherent structures and transport behaviour. Due to the lack of understanding of chaotic advection in three-dimensional flows fundamental studies are necessary.

We study the three-dimensional Reoriented Potential Mixing (3DRPM) flow as a case study for three-dimensional potential flows with chaotic advection. The flow consists of a periodically reoriented dipole flow inside a sphere. This flow is chosen since it is the simplest extension of the 2DRPM flow to three dimensions. The 2DRPM flow has been studied in detail [4, 6, 9]. The natural question is whether the addition of a third dimension has a significant impact on the transport dynamics. It has been observed that even this simple extension of the two-dimensional flow can yield fundamentally different behaviour [5, 8]. In particular the addition of a third dimension means periodic points become periodic lines which yields more complex behaviour.

The 3DRPM Flow

The Steady Dipole Flow

The steady dipole flow forms the basis for the time-dependent reoriented flow. The flow is driven by a source/sink pair located at $(0,0,\pm1)$. While the steady dipole flow in two-dimensions possessed a separating streamline coinciding with the unit circle, this is not the case for the three-dimensional flow. We therefore confine the flow to the unit sphere Ω and use a slip boundary condition. The steady flow is an axisymmetric potential flow, admitting an axisymmetric Stokes stream-function Ψ. Due to this axisymmetry it is natural to use cylindrical coordinates (ρ,θ,z). As outlined in [5, 8], analytic expressions can be found for the flow potential Φ, velocity $\mathbf{v} = \nabla\Phi$ and axisymmetric Stokes stream-function Ψ satisfying $\mathbf{v} = \nabla \times (\Psi/\rho)\hat{\mathbf{e}}_\theta$. Contours of Φ and Ψ are shown in Figure 1 together with the velocity field $\mathbf{v}$. Particle streamlines are the intersections of
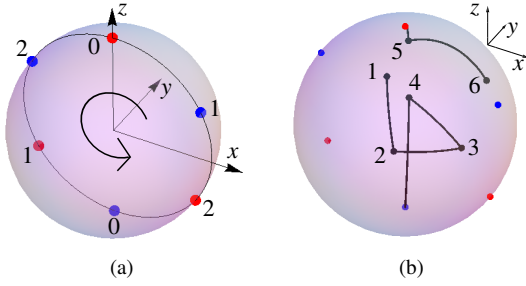
Figure 2. (a) Reorientation protocol for $\Theta = 2\pi/3$. Dipole pairs are labelled according to the number of reorientations of the base flow modulo 3. (b) A typical particle trajectory for the protocol $(\tau, \Theta) = (0.3, 2\pi/3)$.

the isosurfaces of Ψ with planes of constant azimuthal angle θ. These streamlines are illustrated in Figure 1b as the solid lines on the surfaces.

In this study we create a closed flow by enforcing a reinjection protocol at the source/sink. We specify that particles that reach the sink are immediately reinjected at the source along the same streamline. An advantage of our protocol is that Lagrangian structures are preserved during the reinjection process.

We use $\hat{Y}_t$ to denote the solution of the advection equation (1) in the Lagrangian frame, describing streamlines as functions of time from an initial condition $\mathbf{X}$. The map $\hat{Y}_t$ satisfies

$$\hat{Y}_0(\mathbf{X}) = \mathbf{X}, \text{ and } \frac{d}{dt}\hat{Y}_t(\mathbf{X}) = \mathbf{v}\big(\hat{Y}_t(\mathbf{X})\big) \qquad (2)$$

where $\mathbf{X}$ denotes Lagrangian coordinates.

We track particles within the steady dipole flow by numerically integrating equation (1). Since the velocity $\mathbf{v}$ is incompressible, it follows that the map $\hat{Y}_t$ is volume preserving. It is therefore important that our numerical integration scheme is explicitly volume preserving to ensure that Lagrangian structures are preserved. To ensure accuracy we use a fourth order Gauss-Legendre method in conjunction with the method of Finn and Chacón [2].

The Transient Flow

We create a time-dependent flow by periodically reorienting the steady dipole flow. We consider only the simplest reorientation protocol - rotation of the dipole about the y-axis - since it is the most natural extension of the 2DRPM flow. During a time period τ the dipole is active. At the end of τ the dipole is rotated about the y-axis by the angle Θ. Figure 2a shows the dipole positions for $\Theta = 2\pi/3$. The reorientation period τ is non-dimensionalised such that $\tau = 1$ corresponds to the emptying time of the dipole flow, i.e. the time it takes for all fluid in the sphere to pass through the sink.

The velocity field in the transient flow can be approximated by the inertialess piecewise-steady velocity

$$\tilde{\mathbf{v}}(\mathbf{x}, t) = \mathbf{v}\big(R^y_{\lfloor \frac{t}{\tau} \rfloor \Theta} \cdot \mathbf{x}, t\big) \qquad (3)$$

where R^y_β is the rotation matrix corresponding to rotation through the angle β about the y-axis. This approximation is justified in [5, 8].

In this study we primarily use a rotation angle of $\Theta = 2\pi/3$, but our results are generic for all rotation angles of the form $\left(\frac{m}{n}\right)2\pi$ where n is odd. When n is even or irrational different phenomena are observed.
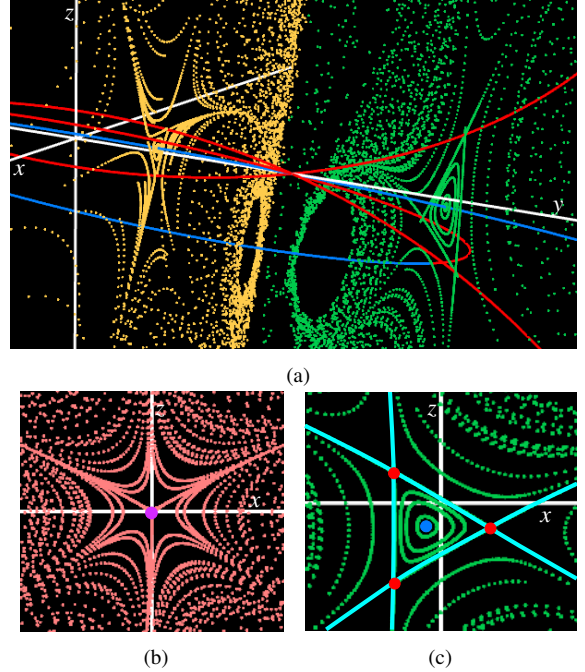

(a)

(b)   (c)

Figure 3. (a) The intersection of three period-3 lines (red, hyperbolic), a period-1 line (blue, elliptic) and the y-axis at a degenerate point. Poincaré sections (yellow, green) are shown for two sets of planar initial conditions, chosen perpendicular to the y-axis. The protocol used is $(\Theta, \tau) = (\frac{2\pi}{3}, 1.1\tau_0)$. (b), (c): Projections of Poincaré sections onto the xz-plane. (b) Initial conditions starting in a plane perpendicular to the y-axis centred around the degenerate point (purple). (c) The green Poincaré section shown in (a). Three hyperbolic lines and one elliptic line intersect the plane (red and blue points). The stable and unstable manifolds are also shown (light blue), forming heteroclinic connections.

For convenience we track particles in the dipole frame. Instead of rotating the dipole after each time period τ we counter-rotate the particles about the dipole. The resulting flow is identical.

Poincaré Sections

A useful tool for the analysis of mixing is Poincaré sections. They express the long time dynamics of a flow. For periodic flows a Poincaré section is created by seeding a number of particles and recording their positions at the end of each flow period. For the particle trajectory shown in Figure 2b the Poincaré section would consist of the points 1,4,7,... when the dipole returns to its starting position. By sectioning in time we reduce the dimension of the system by one, making visualisation simpler.

When a large number of flow periods are used to generate Poincaré sections they reveal both non-mixing and mixing regions. Non-mixing regions appear as circular/toroidal structures and mixing regions appear as a chaotic sea. Both types of regions can be seen in Figure 3.

The mapping of a particle from the end of one flow period to the end of the next is known as the Poincaré map. For the trajectory shown in Figure 2b the Poincaré map would map the positions 1 to 4, 4 to 7 etc. Since we track particles in the dipole frame, the Poincaré map Y consists of advection by the steady dipole flow followed by counter-rotation of the particle, i.e.

$$Y^\Theta_\tau(\mathbf{x}) = R^y_{-\Theta}\hat{Y}_\tau(\mathbf{x}). \qquad (4)$$

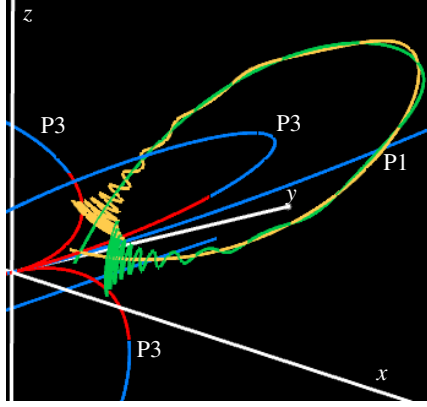The successive iterations of the Poincaré map yields the Poincaré section.

Figure 4. The stable (green) and unstable (yellow) manifolds for a hyperbolic period-3 point on a period-3 line for $\tau = \tau_0$. Three period-3 (P3) lines and one period-1 (P1) line are shown and coloured according to stability (blue-elliptic, red-hyperbolic). Their tangent intersection at the origin is a degenerate point.
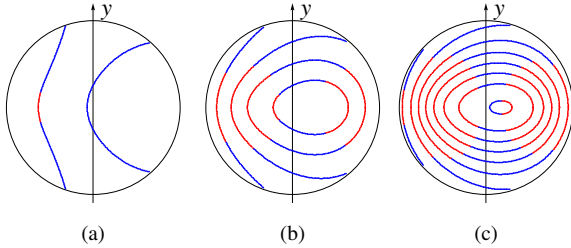

Figure 5. Period-1 lines in the symmetry plane. Elliptic (blue) and hyperbolic (red) segments are highlighted. Degenerate points occur at the intersections of the period-1 lines and the y-axis. (a) $\tau = 0.328$ (b) $\tau = 1.31$ (c) $\tau = 2.62$

Periodic Points and Coherent Structures

Periodic Points and Lines

Periodic point analysis provides a framework for the study of mixing within a flow. Periodic points are classified according to their local stability as determined by the deformation tensor

$$DY(\mathbf{X}) = \left(\frac{\partial Y^i}{\partial X^j} \right) \Big|_{\mathbf{X}} \qquad (5)$$

and its eigenvalues λ_i. The deformation tensor measures how an infinitesimal box of points surrounding a point is deformed by the map Y. Since the flow is incompressible the product of the eigenvalues of the deformation tensor must equal 1.

If $|\lambda_i| = 1$ but at least one eigenvalue is not equal to one then there is rotation but no stretching of local fluid elements and the point is called elliptic. Elliptic points are locally stable and are enclosed by a KAM island or KAM tube that forms an impenetrable barrier to transport. In the case that all the eigenvalues are equal to one the point is called degenerate and there is only shearing of fluid elements.

If $|\lambda_i| > 1$ for some eigenvalue(s) then fluid elements are stretched in the direction of the corresponding eigenvector(s), and contracted in the direction of the eigenvectors corresponding to $|\lambda_i| < 1$. These points are called hyperbolic and are locally unstable. Associated with hyperbolic points are two structures called the stable and unstable manifolds. The stable manifold is the set of points whose trajectories forward in time converge to the hyperbolic point, and the unstable manifold consists of the points whose trajectories backwards in time converge to

the hyperbolic point. They can be computed numerically by seeding a number of particles along the corresponding eigenvector and advecting forward in time for the unstable manifold and backward in time for the stable manifold. Intersections of unstable and stable manifolds are a key indicator of chaos and are called homoclinic connections if the stable/unstable manifolds are associated to the same hyperbolic point, and heteroclinic connections if the manifolds come from different points. The connections can either be transverse or parallel, as shown in Figure 4 and Figure 3c. A single transverse intersection implies infinitely many and provides a mechanism for the stretching and folding of fluid elements that characterises chaotic advection.

If $\lambda_i = 1$ for one of the eigenvalues, then it can be shown that the periodic point forms part of a continuous line of periodic points, with the corresponding eigenvector giving the direction of the continuation of the line. For elliptic points on periodic lines the eigenvalues must be of the form $\lambda_{1,2} = e^{\pm i\omega}$, $\lambda_3 = 1$, where ω gives the rate of rotation about the elliptic point.

When analysing periodic points, a useful quantity is the 'fixed point index' [3]. It can be computed by forming a closed curve around the periodic point and calculating the number of counter-clockwise rotations of the velocity vector in one counter-clockwise traverse of the loop. For example hyperbolic points have index -1 and elliptic points have index $+1$. The sum of fixed point indices is preserved under continuous deformation of a flow, allowing the annihilation and creation of periodic points.

The method used to locate periodic points and lines exploits flow symmetries that are outlined in our previous work [5, 8]. Coherent structures must be symmetric about the symmetry plane $z = \tan(-\Theta/2)x$. We can therefore restrict the initial search for odd order periodic points to the symmetry plane, making computation significantly easier. Once periodic points are found, the deformation tensor is numerically evaluated using a second order finite difference approximation for the derivatives to determine the stability of the point. If one of the eigenvalues of the deformation tensor is equal to one, then we know the periodic point forms part of a line and use the direction of the associated eigenvector to search for another point on the line that is a fixed distance away. Figure 5 shows the period-1 lines and their stability for a sequence of τ values. In all cases considered so far all periodic points in the 3DRPM flow have been part of periodic lines and no isolated periodic points have been found.

Degenerate Points: an Inhibitor to Chaos

In this section we show that degenerate periodic points in the 3DRPM flow create stable elliptic regions making global chaos impossible. This result is generic to all flows with the same type of degenerate periodic points, inhibiting the extent of chaos.

In the 3DRPM flow degenerate points appear when a period-1 line intersects the y-axis. Figure 5 shows that they accumulate as τ increases. The degenerate points are special because when viewing the flow in the laboratory frame they return to their initial positions after each phase of the steady dipole flow, not just when the dipole returns to its starting position. In each phase of the flow local fluid elements are sheared, but the net shear at the end of the flow period is zero. Since there is no net local deformation of fluid elements the deformation tensor is equal to the identity matrix. At such points for $\Theta = 2\pi/3$ there are three unstable and three stable directions as shown in Figure 3b. For general odd rotation angles $\Theta = 2\pi\frac{m}{n}$ there will be n stable and n unstable directions equally spaced apart by an angle π/n and alternating between stable and unstable.

Direct computation of the fixed point index for the degenerate points gives an index of -2 for the $\Theta = 2\pi/3$ case. For general odd rotations the index is $1 - n$. In the local vicinity of the degenerate point the period-1 line is elliptic except at the degenerate point. To preserve the fixed point index of -2 three hyperbolic period-3 lines also intersect at the degenerate point, as seen in Figure 3a. Each period-3 line is hyperbolic except at the degenerate point. This is not the only topological possibility, for example two hyperbolic periodic lines could intersect at the degenerate point, but we observe nothing else in the 3DRPM flow. Figure 3c shows how the elliptic and hyperbolic points arrange themselves and create an essentially 2D flow in the local region. The unstable and stable manifolds associated with the hyperbolic period-3 points form parallel heteroclinic connections that bound the KAM tube associated with the elliptic period-1 point. Each KAM tube is an impenetrable barrier to fluid transport.

In the vicinity of the y-axis the period-1 lines are elliptic except at the degenerate point, degeneracies therefore occur when the local rotation rate ω given by the deformation tensor DY_τ^Θ becomes zero. Figure 6 shows the local rotation rate ω at distances d along the period-1 line for a range of τ values. The distance d is measured from the xz-plane. The left-right symmetry in Figure 6 is expected since transport in the y^+ and y^- hemispheres mirror each other [8]. The degenerate points are those for which $\omega = 0$ and are shown as the large points in Figure 6. The magnitude of the rotation rate ω increases further away from the degenerate point, causing an increase in the size of the stable KAM tube.

It can also be seen from Figure 6 that there is a critical τ value τ_0 such that there is exactly one degenerate point on the period-1 line. Computation shows that $\tau_0 \approx 0.29344$. For values of τ greater than τ_0 there are two degenerate points and for τ less than τ_0 there are none. The value τ_0 therefore corresponds to a local flow bifurcation. For $\tau > \tau_0$ the three period-3 lines, the period-1 line and the y-axis intersect transversely at the degenerate point. This creates a reversal in the orientation of coherent structures, illustrated in Figure 3a, and a change in the sign of the rotation rate as seen in Figure 6. For $\tau = \tau_0$ the three period-3 lines, the period-1 line and the y-axis form a tangent intersection. In this case the rate of rotation does not change sign and so there is no reversal in orientation of coherent structures.

At $\tau = \tau_0$ the first degenerate point is created. The number of degenerate points increases with τ and each degenerate point creates a small stable region. Therefore global chaos will only be possible for $\tau < \tau_0$. However it has been observed that there are KAM tori associated with period-1 lines for all $\tau < \tau_0$, making global chaos in the 3DRPM flow impossible.

Conclusions

Degenerate points in chaotic flows have not been studied in detail in the past. In this paper we have shown that they play a significant role in the global transport dynamics of flows. Their existence can result in stable elliptic regions that form impenetrable barriers to transport. For the 3DRPM flow the overall degree of disorder increases with τ, yet the increasing number of degenerate points and associated stable elliptic regions makes global chaos impossible. Flows with the same type of degenerate points will exhibit the same phenomena making them unsuitable for mixing applications. However, the stable regions could be beneficial for processes in which isolation of fluid is desired, such as contaminant extraction from groundwater.

The full impact of the degenerate points has not yet been explored. The topological shifts in the number of degenerate points and the stable/unstable manifolds associated with the
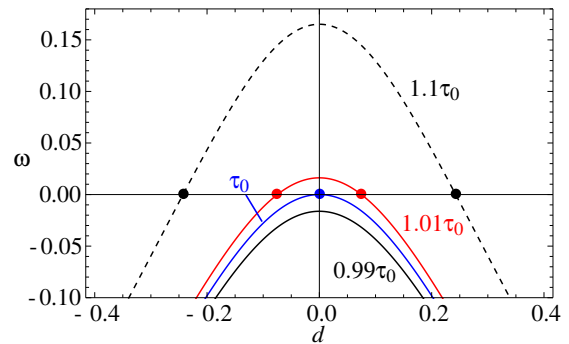

Figure 6. The local rotation rate ω given by the deformation tensor at points a distance d along the period-1 line from the xz-plane. Curves are shown for $\tau = 0.99\tau_0, \tau_0, 1.01\tau_0, 1.1\tau_0$. Degenerate points are marked by large dots, where $\omega = 0$.

period-3 lines that pass through the degenerate point could have a significant impact on transport organisation.

Future work should consider more complex reorientation protocols in order to break the flow symmetries that create the degenerate points and associated stable regions. A small perturbation of the axis of dipole rotation away from the y-axis might be all that is needed to generate global chaos.

*

References

[1] Bajer, K., Hamiltonian Formulation of the Equations of Streamlines in Three-dimensional Steady Flows, *Chaos, Solitons & Fractals*, **4**, 1994, 895–911.

[2] Finn, J. M. and Chacón, L., Volume preserving integrators for solenoidal fields on a grid, *Phys. Plasmas*, **12**, 2005, 054503.

[3] Katok, A. and Hasselblatt, B., *Introduction to the Modern Theory of Dynamical Systems*, Cambridge University Press, 1996.

[4] Lester, D. R., Rudman, M., Metcalfe, G., Trefry, M. G., Ord, A. and Hobbs, B., Scalar dispersion in a periodically reoriented potential flow: Acceleration via Lagrangian chaos, *Phys. Rev. E*, **81**, 2010, 046319.

[5] Lester, D. R., Smith, L. D., Metcalfe, G. and Rudman, M., Beyond Hamiltonian: Chaotic Advection in a Three-Dimensional Volume Preserving Flow, in *Proc. 9th Int. Conf. on CFD in the Minerals and Process Industries*, 2012.

[6] Metcalfe, G., Lester, D. R., Ord, A., Kulkarni, P., Rudman, M., Trefry, M. G., Hobbs, B., Regenauer-Lieb, K. and Morris, J., An experimental and theoretical study of the mixing characteristics of a periodically reoriented irrotational flow, *Phil. Trans. R. Soc. A*, **368**, 2010, 2147–2162.

[7] Ottino, J. M., *The kinematics of mixing: stretching, chaos, and transport*, Cambridge University Press, 1989.

[8] Smith, L. D., Lester, D. R. and Metcalfe, G., Chaotic Advection in a Three-Dimensional Volume Preserving Potential Flow, in *Proc. 18th AFMC*, 2012.

[9] Trefry, M. G., Lester, D. R., Metcalfe, G., Ord, A. and Regenauer-Lieb, K., Toward enhanced subsurface intervention methods using chaotic advection, *J. Contam. Hydrol.*, **127**, 2012, 15–29.

[10] Wiggins, S., Coherent structures and chaotic advection in three dimensions, *J. Fluid Mech.*, **654**, 2010, 1–4.